

REGULAR PAPER • OPEN ACCESS

## Argon gas flow through glass nanopipette

To cite this article: Tomohide Takami *et al* 2016 *Jpn. J. Appl. Phys.* **55** 125202

View the [article online](#) for updates and enhancements.

You may also like

- [New Method in Surface Treatment of Nanopipette for Interface between Two Immiscible Electrolyte Solutions \(ITIES\) Experiment](#)  
Edappalil Satheesan Anupriya and Mei Shen
- [Development of a probing system for a micro-coordinate measuring machine by utilizing shear-force detection](#)  
So Ito, Issei Kodama and Wei Gao
- [Review—Nanopipette Applications as Sensors, Electrodes, and Probes: A Study on Recent Developments](#)  
Kaan Kececi, Ali Dinler and Dila Kaya



## Argon gas flow through glass nanopipette

Tomohide Takami<sup>1\*</sup>, Kiwamu Nishimoto<sup>2</sup>, Tadahiko Goto<sup>2</sup>, Shuichi Ogawa<sup>2</sup>, Futoshi Iwata<sup>3</sup>, and Yuji Takakuwa<sup>2</sup>

<sup>1</sup>Division of Liberal Arts, Kogakuin University, Hachioji, Tokyo 192-0015, Japan

<sup>2</sup>Institute of Multidisciplinary Research for Advanced Materials (IMRAM), Tohoku University, Sendai 980-8577, Japan

<sup>3</sup>Faculty of Engineering, Shizuoka University, Hamamatsu 432-8561, Japan

\*E-mail: takami@cc.kogakuin.ac.jp

Received September 2, 2016; accepted September 15, 2016; published online November 11, 2016

We have observed the flow of argon gas through a glass nanopipette in vacuum. A glass nanopipette with an inner diameter of 100 nm and a shank length of 3 mm was set between vacuum chambers, and argon gas was introduced from the top of the nanopipette to the bottom. The exit pressure was monitored with an increase in entrance pressure in the range of 50–170 kPa. Knudsen flow was observed at an entrance pressure lower than 100 kPa, and Poiseuille flow was observed at an entrance pressure higher than 120 kPa. The proposed pressure-dependent gas flow method provides a means of evaluating the glass nanopipette before using it for various applications including nanodeposition to surfaces and femtoinjection to living cells. © 2016 The Japan Society of Applied Physics

### 1. Introduction

Glass nanopipettes have been used as a bridge between the macroworld and the nanoworld.<sup>1)</sup> Pipettes have been used as a tool for transferring liquids with various volumes,<sup>2)</sup> and many novel phenomena and applications are obtained as the size of pipettes decreases to micro- or nanometers. For example, glass pipettes were used to obtain the ionic currents flowing through a cell's plasma membrane in the patch clamp technique.<sup>3,4)</sup> The low-volume liquid delivery induced by an electric field was realized and used for nanofluidics and nanolithography, which were essential for controlled delivery and selective deposition.<sup>5–8)</sup> Nanopipettes could also be used as probes in scanning electrochemical microscopy (SECM) and scanning ion conductance microscopy (SICM) for high-resolution imaging.<sup>9–11)</sup> The ion transfer process and its kinetic parameters at a liquid/liquid interface were studied using nanopipettes.<sup>12)</sup> Ion current rectification (ICR) is a specific phenomenon occurring in nanopipettes.<sup>13)</sup> Deng et al. reported the dependence of ICR on the concentration gradient of KCl solutions in polyethyleneimine-modified glass nanopipettes.<sup>14)</sup> Yuill et al. demonstrated the application of nanopipettes as electrospray ionization emitters for mass spectrometry.<sup>15)</sup> Moreover, microinjection is a useful method of transfection to cells,<sup>16)</sup> and the viability of cells after the microinjection is not sufficiently high to obtain statistical and quantitative results.<sup>17)</sup>

These studies require the control of the diameter and inside cleanness of the nanopipettes.<sup>13,14)</sup> Ionic current strongly depends on the inner diameter of the nanopipettes. Nanofluidics and nanolithography require cleanness inside the nanopipettes.<sup>5–8)</sup> The stable current through the nanopipettes is preferable for imaging by SECM and SICM.<sup>9–11)</sup> One of the important key technologies to achieve a high viability for microinjection is the constant reproduction of injection micropipettes.<sup>16,17)</sup> Therefore, the evaluation of the condition of nanopipettes is necessary for the stable use of nanopipettes for these studies.

However, the evaluation of prepared nanopipettes with an optical microscope is beyond Abbe's resolution limit. Scanning electron microscopy (SEM) enables us to observe

the top of nanopipettes, although the samples should be electrically conductive so that metal or ionic liquid can be deposited on the samples, and deposited nanopipettes cannot be used after SEM observation. Moreover, a destructive measurement is unavoidable for imaging the inner part of a glass nanopipette with SEM. Therefore, a nondestructive and contamination-free measurement is required for the evaluation of nanopipettes before their use. A conventional way to inspect glass micropipettes before their use is to dip their tip in a liquid and apply air pressure to the wider entrance to observe the bubbles from the tip, although it cannot be applied to nanopipettes because their inner diameter is too small to observe bubbles.

Although gas flow through nanoholes has already been investigated,<sup>18)</sup> gas flow through nanopipettes has not been reported yet as far as we know. In this paper, we propose a new nondestructive gas flow method to test glass nanopipettes before using them for microinjection. We observe the exit gas pressure of nanopipettes by changing the entrance pressure of argon gas from 50 to 170 kPa. We also use various rare-gas atoms in this experiment in order to know how the atomic radius and viscosity are affected by the flow through a glass nanopipette and what rare-gas atom is suitable for the evaluation of the nanopipettes.

### 2. Experimental methods

We introduced a glass nanopipette into a vacuum chamber and measured the vacuum conductance through the nanopipette, as shown schematically in Fig. 1. Since the gas flow rate through the nanopipette was too low to measure using the mass flow controller, the entrance and exit pressures were observed. The entrance pressure was varied in the range of 50–170 kPa. The inner diameter of the nanopipette used in this study was confirmed to be 100 nm from the SEM image shown in Fig. 1. The shank length of the nanopipette was observed to be ca. 3 mm using an optical microscope.

The nanopipette was fabricated from boron silicate capillary tubes (Narishige GD-1; outer diameter: 1.0 mm; inner diameter: 0.6 mm) using a puller (Sutter P-2000) at Shizuoka University. The preparation method was written in detail in previous reports.<sup>19–22)</sup> The nanopipette was attached



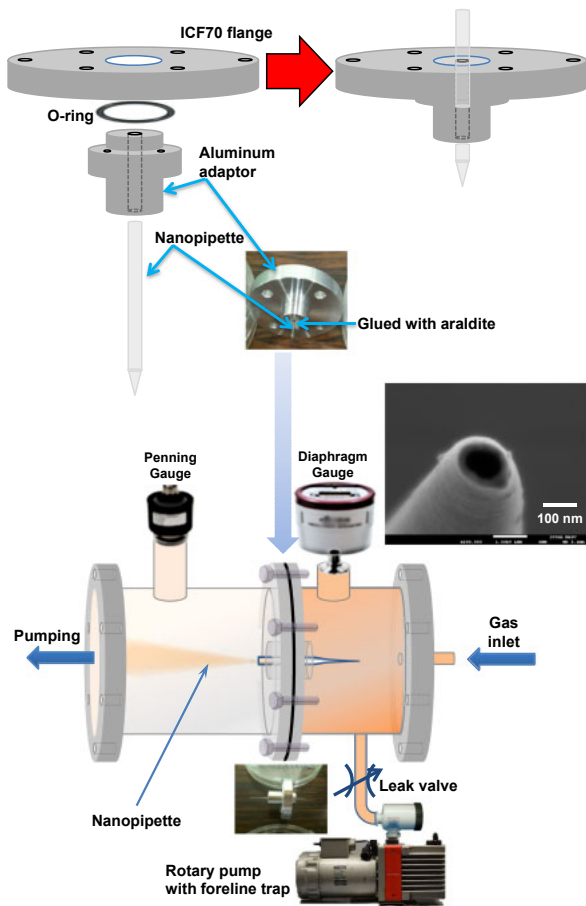


**Fig. 1.** (Color online) Schematic drawing of the apparatus. The nanopipette with a top inner diameter of 100 nm, as shown in the SEM image on the middle right, was fixed at the center of an adaptor and set between two vacuum chambers. The flow of the inlet gas was controlled with a mass flow controller, and the entrance pressure to the nanopipette was controlled with a leak valve connected to a rotary pump with a foreline trap, and monitored with a diaphragm gauge. The exit pressure was monitored with a Penning gauge.

to a pin through-hole adaptor using araldite and the adaptor was connected to a 70-mm- $\phi$  flange, as shown schematically in Fig. 1, and the flange was set between two vacuum chambers. The base pressure of these vacuum chambers was constantly kept below  $1.0 \times 10^{-4}$  Pa. To measure the vacuum conductance of the nanopipette, argon gas (purity: >99.999%) was allowed to flow from the top of the nanopipette to the bottom. The leak of the gas line was examined using a mass spectrometer (MKS e-Vision). The entrance pressure of the nanopipette was controlled using a leak valve connected to a rotary pump using a foreline trap, and measured using a diaphragm gauge (MKS 622). The exit pressure was measured using a Penning gauge (Leybold PR28), a hot-filament ionization gauge (ULVAC WIN-N3), and a mass spectrometer (Pfeiffer PrismaPlus QMG220M2). After the experiment, we measured the top diameter of the nanopipette by field-effect scanning electron microscopy (JEOL JSM-7800F and Hitachi S-4800) for confirmation. The typical SEM image of the nanopipette is shown in Fig. 1, and we confirmed that the nanopipette did not change during the experiment.

Figure 2 shows the typical data for the estimation of the vacuum conductance through the nanopipette. Since the gas flow through the nanopipette was too small to observe with a

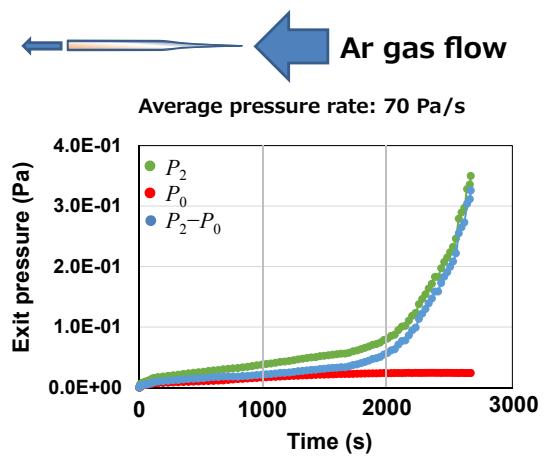


**Fig. 2.** (Color online) Time evolution of the pressure at the exit chamber.  $t = 0$  is the time when the gate valve between the exit chamber and the pump was closed. Green curve: argon gas was introduced into the entrance chamber at  $t = 0$  with an average increasing pressure rate of 70 kPa/s, so that the time dependence of the exit pressure ( $P_2$ ) was observed. Red curve: time dependence of the base pressure, without introducing the argon gas to the entrance chamber, so that the time dependence of the base pressure at the exit pressure ( $P_0$ ) was observed. Blue curve: the subtraction  $P_2 - P_0$ .

flow meter, we applied a gas storage method to measure the tiny gas flow as follows. First, the gate valve of the exit chamber was closed and then argon gas was introduced into the entrance chamber to observe the entrance pressure ( $P_1$ ) dependence of the exit pressure. Therefore, the pumping speed of the exit chamber ( $S$ ), estimated to be ca. 7 L/s, can be neglected and the observed exit pressure  $P_2$  can be estimated from

$$V \frac{dP_2}{dt} + Q = C(P_1 - P_2), \quad (1)$$

where  $V$  is the volume of the exit chamber, estimated to be 1.67 L,  $Q$  is the parameter depending on the outgas and leak speed and pumping speed of the Penning gauge behaving like an ion pump, and  $C$  is the conductance through the nanopipette. The green curve in Fig. 2 shows the time-dependent exit pressure  $P_2$  with an increase in entrance argon gas pressure at an average rate of 70 Pa/s. The point  $t = 0$  corresponds to the time when the gate valve of the exit chamber was closed and then argon gas was introduced into the entrance chamber. Second, the gate valve of the exit chamber was closed but no argon gas flow was introduced into the entrance chamber to estimate  $Q$  from

$$V \frac{dP_0}{dt} + Q = 0, \quad (2)$$

where  $P_0$  is the exit pressure with no argon gas flow introduced into the entrance chamber. The red curve in Fig. 2 shows the time-dependent exit pressure  $P_0$  with no argon gas introduced into the entrance chamber. The point  $t = 0$  corresponds to the time when the gate valve of the exit chamber was closed. The blue curve in Fig. 2 shows the value of  $P_2 - P_0$ . With Eqs. (1) and (2), the following equation was obtained:

$$C = \frac{V}{P_1 - P_2} \frac{d(P_2 - P_0)}{dt}. \quad (3)$$

From this equation,  $C$  was estimated. Since the value of  $P_1 - P_2$  in Eq. (3) decreases at  $P_1$  values less than 50 kPa, the

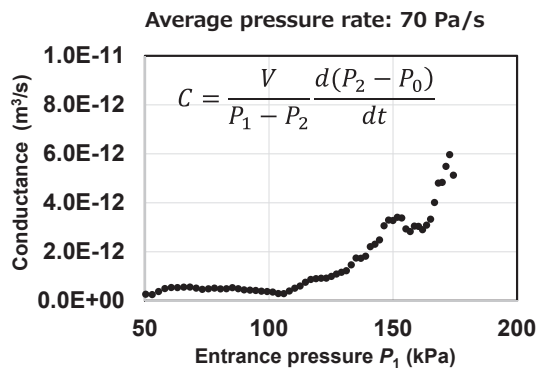


Fig. 3. Vacuum conductance dependence on the entrance pressure ( $P_1$ ), estimated from the data shown in Fig. 2 ( $P_2 - P_0$ ) with Eq. (3) in the text, shown in the graph. Five-point data smoothed.

plot data of the vacuum conductance less than 50 kPa are not shown in this paper owing to the large errors of the estimated values.

The leakage between the entrance and exit chambers was measured by caulking the wider end of the nanopipette set between the chambers with araldite. Using helium gas, the leakage pressure at the exit chamber was determined to be less than  $3.0 \times 10^{-5}$  Pa when the entrance chamber pressure (He gas) was 170 kPa.

### 3. Results

Figure 3 shows a curve of the dependence of the vacuum conductance ( $C$ ) of the glass nanopipette on the entrance pressure  $P_1$ . This curve is estimated from the subtracted pressure ( $P_2 - P_0$ ) curve (blue) in Fig. 2, using Eq. (3). In the entrance pressure range of  $50 \text{ kPa} < P_1 < 100 \text{ kPa}$ , the dependence of the vacuum conductance is almost flat, which indicates that the almost flat dependence region corresponds to the Knudsen flow.<sup>23)</sup> In the entrance pressure range of  $120 \text{ kPa} < P_1 < 170 \text{ kPa}$ , the dependence of the vacuum conductance is positive, which indicates that the positive dependence region corresponds to the Poiseuille flow.

The observed curve can be roughly fitted with the following Knudsen's equation:<sup>23)</sup>

$$C = \frac{\pi D^4}{128 \eta L} P + \frac{1}{6} \sqrt{\frac{2\pi RT}{M}} \frac{D^3}{L} \frac{1 + \sqrt{\frac{M}{RT}} \frac{DP}{\eta}}{1 + 1.24 \sqrt{\frac{M}{RT}} \frac{DP}{\eta}}, \quad (4)$$

where  $D$  is the inner diameter of the nanopipette (ca. 100 nm in this study),  $L$  is the length of the nanopipette at a small area (ca. 3 mm in this study),  $T$  is the temperature,  $M$  is the mass of the rare-gas atom (kg/mol),  $R$  is the gas constant, and  $\eta$  is the viscosity (Pa·s) that can be estimated from the values indicated in Ref. 24. However, the estimated temperature by fitting the experimental data using Eq. (4) was approximately 7 K, and we could not observe the vacuum conductance in the cases of Kr and Xe gases at such a low temperature, which indicates that Eq. (4) is not suitable for estimating nanopipette conductance. Therefore, in order to estimate the tip diameter of the nanopipette, we should consider the shape of the conical tube (nanopipette) in the following way shown in the next paragraph.

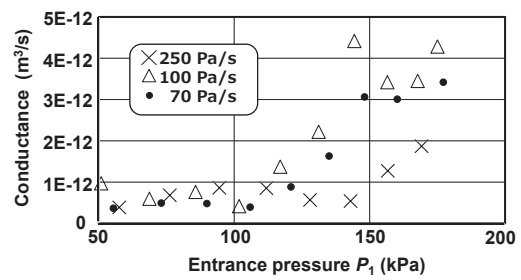


Fig. 4. Vacuum conductance dependence on the entrance pressure, with the average increasing pressure rates of 250 (x), 100 ( $\Delta$ ), and 70 ( $\bullet$ ) kPa/s. All the data points were thinned for the comparison of the data.

In the almost flat dependence region (Knudsen flow) in Fig. 3, the average conductance is  $5.0 \times 10^{-13} \text{ m}^3/\text{s}$ . The theoretical vacuum conductance of air (mean molecular mass 29) through the conical tube in the Knudsen region can be estimated from

$$C = 121 \frac{D_1^2 D_2^2}{(D_1 - D_2)L/2}, \quad (5)$$

where  $D_1$  and  $D_2$  are the entrance and exit of the cone (nanopipette shank), respectively, and  $D_2 = 0.60 \text{ mm}$  in this study.<sup>25)</sup> In the case of argon gas (atomic mass: 40), we converted the value 121 in Eq. (5) into  $121 \times (29/40)^{1/2} = 103$  since the mean velocity of gas is proportional to  $M^{-2}$ .<sup>25,26)</sup> The observed conductance in the Knudsen flow region shown in Fig. 3 is  $5.0 \times 10^{-13} \text{ m}^3/\text{s}$ , such that  $D_1$  is estimated to be  $1.0 \times 10^2 \text{ nm}$ , which is fairly in agreement with the value obtained from the SEM image shown in Fig. 1. In this way, the inner diameter of the glass nanopipette can be estimated from the vacuum conductance, which provides a nondestructive method to inspect nanopipettes before their use.

### 4. Discussion

Figure 4 shows the dependence of the conductance on the entrance pressure with increasing pressure rate. In the Knudsen flow region, the conductances are almost the same even with increasing pressure rates of 70, 100, and 250 Pa/s. On the other hand, the conductance depends on the average pressure rate, which is attributed to the nonsteady flow of argon gas in the Poiseuille flow region.

When the nanopipette was set in the opposite way, i.e., introducing the gas flow from the wider end and effusing it to the tip of the nanopipette, the pressure dependence changed, as shown in Fig. 5. The minimum conductances were observed at around 100 and 80 kPa at the average pressure rates of 100 and 220 Pa/s, respectively. The pressure dependence shown in Fig. 5 was different from that shown in Fig. 3; the local maximum was observed at ca. 50 kPa. Sugimoto et al. observed the nonsteady molecular flow in the microcapillary array (MCA; 6  $\mu\text{m}$  channel diameter and 59% aperture ratio) during the initial gas flow, and the nonsteady molecular flow obeys a diffusion equation.<sup>27)</sup> They also indicated that the time of flight in the MCA determines the time response in the case of argon gas where the dwelling time on the inner capillary surface is short. Their results are in agreement with those of our study shown in Fig. 5, and we consider that the negative dependence and instability of the conductances at less than 80 kPa are attributed to the

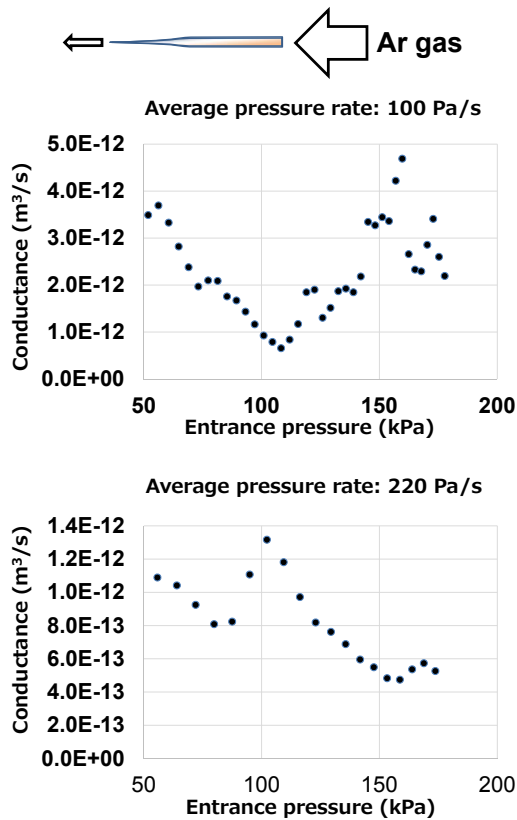


**Fig. 5.** (Color online) Vacuum conductance dependence on the entrance pressure in the case that the gas flow was introduced from the wider end to the top, as shown schematically in the upper figure. Upper and lower graphs: average pressure rates of 100 and 220 Pa/s, respectively.

nonsteady molecular flow. Moreover, we simulated the pressure distribution in the nanopipette and compared the gas flow from the tip to the wider end at the opposite end. In the case of the gas flow from the tip to the wider end, the distribution drastically changed around the entrance of the top of the nanopipette, whereas the pressure rate was not so high after the gas entered from the top. This gas flow geometry resembles a skimmer for obtaining stable molecular beams.<sup>28)</sup>

On the other hand, in the case of the gas flow from the wider end to the top, the distribution did not change markedly at the entrance; however, the pressure rapidly changed around the exit top of the nanopipette, which might have caused turbulence in the nanopipette. Note that the frequency of clogging the nanopipette is more than ten times when the gas flows from the wider end to the top than the opposite flow, owing to the hardly unavoidable dust in the vacuum chamber.

Sakagami measured the vacuum conductance of glass capillaries.<sup>29)</sup> The shank length was around 50 mm, the inner diameter of the capillary was 0.8 mm, and the top diameter was 2.5–27 μm. The top inner diameter of the capillaries used in their study was one or two order higher than those used in this study. Therefore, the conductances estimated in their study were  $5.94 \times 10^{-11}$ – $4.06 \times 10^{-8}$  m³/s, which are 2–4 order larger than those observed in this study. In their experiment, the gas flow was introduced into the capillary from the wider end to the top, and it is supposed that the clogging of the capillary during the experiment might have been a problem in their study, which is the reason why we introduced the gas flow from the tip top to the wider end, an opposite flow. We have observed the vacuum conductance of a 1-μm-inner-diameter micropipette with our apparatus. We could not determine the exit pressure with a Penning gauge when the entrance pressure was more than 70 kPa because the exit chamber pressure exceeded 1 Pa. Nevertheless, we have observed a local maximum of the vacuum conductance in the entrance pressure range of 20–30 kPa, which might be due to the nonsteady gas flow in the micropipette. Note that the local maximum was observed in both directions of the gas flow: from the tip top to the wider end and the opposite.

We have also tried various types of rare-gas atoms in this experiment in order to know how the atomic radius and viscosity are affected by the flow through a glass nanopipette and what rare-gas atom is suitable for the evaluation of the nanopipette. Figure 6 shows the dependence of exit vacuum pressure on entrance pressure for a clogged nanopipette, confirmed using an optical microscope, for He, Ne, Ar, Kr, and Xe rare gases. The discontinuous jumps in the graphs

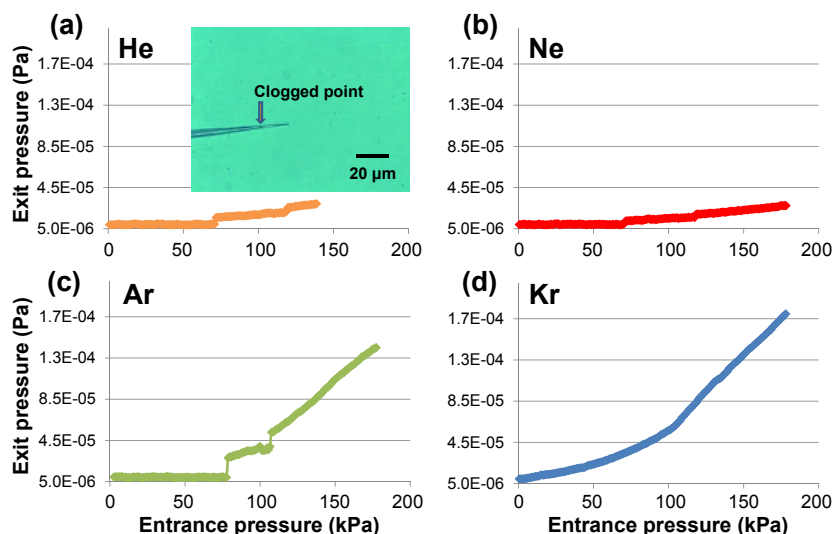


**Fig. 6.** (Color online) Exit pressure dependence on the entrance pressure in the case of a clogged nanopipette, as shown in the optical microscopic image shown on the upper left.

were observed at pressures of ca. 70 and 110 kPa, which was not apparent in the case of krypton. From the reproducible experiments, we found that the pressure dependence was discontinuous when the nanopipette was clogged. The first viscosity virial coefficient for argon, which could be related to the force interaction between the argon atom and other materials, is the highest among those for rare gases.<sup>24)</sup> Thus, we can also check the inner cleanness of the nanopipette by our gas flow method, and argon gas is suitable for checking the inside cleanness of nanopipettes.

The temperature at the tip top part of the nanopipette is difficult to observe even with a thermocouple or radiation thermometer. Actually, even a capillary of micrometer-order diameter could be clogged with frozen H<sub>2</sub>O.<sup>30)</sup> Future study with temperature control at the tip top of the glass nanopipette will solve this problem.

Reynolds number ( $Re$ ) can be estimated using

$$Re = \frac{\rho v D_1}{\eta}, \quad (6)$$

where  $\rho$  and  $v$  are the density and velocity of the gas flowing in the nanopipette, respectively, which could not be estimated in this experimental study; however, the other values could be estimated ( $D_1 = 100$  nm and  $\eta = 22.6$  Pa·s in the case of Ar gas<sup>24)</sup>). Further theoretical study is necessary in order to estimate  $\rho$  and  $v$ .

Finally, we address the extensive prospect of this study. We used rare gases for the evaluation of nanopipettes because they are inert, and charged or polarized molecules could rectify gas flow through charged nanopipettes like ICR in liquid,<sup>14)</sup> which will be a future interesting study of the gas flow through nanospace, related to the study of nanopore sequencing.<sup>31)</sup> Sugimoto et al. observed the long dwelling time of NO gas in a glass capillary and showed that the dwelling time determines the response time and time of flight through the capillary,<sup>27)</sup> which indicates the possibility of rectifying gas flow through charged nanopipettes.

## 5. Conclusions

We have observed the pressure differences between the entrance and exit of a nanopipette for rare gases by changing the entrance stagnation pressure from 50 to 170 kPa. The flow state of the rare gas through the nanopipette transitioned from Knudsen flow to intermediate flow to Poiseuille flow with an increase in entrance pressure. We have proposed a convenient method of estimating the inner diameter of glass nanopipettes without any damage to the nanopipettes. In evaluating nanopipettes, including their inside cleanness, argon gas is the most favorable among rare gases because it works effectively for the evaluation of nanopipettes by the gas-flow method proposed and has the highest nature abundance ratio among rare gases.

We are preparing for further theoretical study of vacuum conductance through nanopipettes, especially for the discussion of an opposite gas flow through nanopipettes, using a dynamic equation,<sup>32–35)</sup> which will be published elsewhere.<sup>36)</sup>

## Acknowledgments

We are grateful to Mr. Hideyuki Magara of the Technical Service Section of IMRAM Tohoku University for the JEOL

SEM observation, and Dr. Takeshi Sugawara of ReMcD, Hiroshima University for the discussion of the theory of vacuum conductance. We also thank Professor Ichiro Arakawa of Gakushuin University, Professor Katsuyuki Fukutani of the University of Tokyo, and Professor Ichiro Takano and Mr. Atsushi Sekiguchi of Kogakuin University for valuable discussions. This work was supported by the Platform for Dynamic Approaches to Living System from the Ministry of Education, Culture, Sports, Science and Technology, Japan, JSPS KAKENHI Grant Number 15K04678. It was also performed under the Cooperative Research Program of the “Network Joint Research Center for Materials and Devices” at IMRAM Tohoku University.

- 1) T. Takami, B. H. Park, and T. Kawai, *Nano Convergence* **1**, 17 (2014).
- 2) C. A. Morris, A. K. Friedman, and L. A. Baker, *Analyst* **135**, 2190 (2010).
- 3) Y. Zhao, S. Inayat, D. A. Dikin, J. H. Singer, R. S. Ruoff, and J. B. Troy, *J. Nanoeng. Nanosyst.* **222**, 1 (2008).
- 4) M. Malboubi, Y. Gu, and K. Jiang, *Microelectron. Eng.* **87**, 778 (2010).
- 5) S. An, C. Stambaugh, G. Kim, M. Lee, Y. Kim, K. Lee, and W. Jhe, *Nanoscale* **4**, 6493 (2012).
- 6) A. P. Suryavanshi and M. F. Yu, *Appl. Phys. Lett.* **88**, 083103 (2006).
- 7) A. P. Suryavanshi and M. F. Yu, *Nanotechnology* **18**, 105305 (2007).
- 8) F. O. Laforge, J. Carpino, S. A. Rotenberg, and M. V. Mirkin, *Proc. Natl. Acad. Sci. U.S.A.* **104**, 11895 (2007).
- 9) C. B. Prater, P. K. Hansma, M. Tortonese, and C. F. Quate, *Rev. Sci. Instrum.* **62**, 2634 (1991).
- 10) Y. Takahashi, A. I. Shevchuk, P. Novak, Y. Murakami, H. Shiku, Y. E. Korchev, and T. Matsue, *J. Am. Chem. Soc.* **132**, 10118 (2010).
- 11) P. Elsamadisi, Y. X. Wang, J. Velmurugan, and M. V. Mirkin, *Anal. Chem.* **83**, 671 (2011).
- 12) Q. Li, S. Xie, Z. Liang, X. Meng, S. Liu, H. H. Girault, and Y. Shao, *Angew. Chem.* **121**, 8154 (2009).
- 13) C. Wei, A. J. Bard, and S. W. Feldberg, *Anal. Chem.* **69**, 4627 (1997).
- 14) X. L. Deng, T. Takami, J. W. Son, E. J. Kang, T. Kawai, and B. H. Park, *Sci. Rep.* **4**, 4005 (2014).
- 15) E. M. Yuill, N. Sa, S. J. Ray, G. M. Hieftje, and L. A. Baker, *Anal. Chem.* **85**, 8498 (2013).
- 16) R. E. Hammer, V. G. Pursel, C. E. Rexroad, Jr., R. J. Wall, D. J. Bolt, K. M. Ebert, R. D. Palminter, and R. L. Brinster, *Nature* **315**, 680 (1985).
- 17) H. Matsuoka, M. Saito, and H. Funabashi, in *Embryonic Stem Cells—Basic Biology to Bioengineering*, ed. M. S. Kallos (InTech, Rijeka, 2011) p. 149.
- 18) M. Savard, C. Tremblay-Darveau, and G. Gervais, *Phys. Rev. Lett.* **103**, 104502 (2009).
- 19) F. Iwata, S. Nagami, Y. Sumiya, and A. Sasaki, *Nanotechnology* **18**, 105301 (2007).
- 20) S. Ito and F. Iwata, *Jpn. J. Appl. Phys.* **50**, 08LB15 (2011).
- 21) T. Takami, F. Iwata, K. Yamazaki, J. W. Son, J.-K. Lee, B. H. Park, and T. Kawai, *J. Appl. Phys.* **111**, 044702 (2012).
- 22) F. Iwata, K. Yamazaki, K. Ishizaki, and T. Ushiki, *Jpn. J. Appl. Phys.* **53**, 036701 (2014).
- 23) M. Knudsen, *Ann. Phys.* **333**, 75 (1909).
- 24) J. Kestin, S. T. Ro, and W. A. Wakeham, *J. Chem. Phys.* **56**, 4119 (1972).
- 25) *Shinku Handbook*, ed. ULVAC Co., Ltd. (Ohmsha, Tokyo, 2002) p. 43 [in Japanese].
- 26) J. F. O'Hanlon, *A User's Guide to Vacuum Technology* (Wiley, Hoboken, NJ, 2003) 3rd ed., p. 25.
- 27) T. Sugimoto, T. Okano, and K. Fukutani, *J. Vac. Soc. Jpn.* **52**, 141 (2009) [in Japanese].
- 28) M. Jugroot, C. P. T. Groth, B. A. Thomson, V. Baranov, and B. A. Collings, *J. Phys. D* **37**, 1289 (2004).
- 29) H. Sakagami, BS Thesis (2005) [in Japanese]. Available online at [www.kochi-tech.ac.jp/library/ron/2004/2004ele/1050220.pdf](http://www.kochi-tech.ac.jp/library/ron/2004/2004ele/1050220.pdf).
- 30) T. Sugimoto and K. Fukutani, private communication.
- 31) C. Dekker, *Nat. Nanotechnol.* **2**, 209 (2007).
- 32) F. Sharipov, *J. Vac. Sci. Technol. A* **14**, 2627 (1996).
- 33) F. Sharipov, *J. Vac. Sci. Technol. A* **15**, 2434 (1997).
- 34) F. Sharipov and V. Seleznev, *J. Phys. Chem. Ref. Data* **27**, 657 (1998).
- 35) F. Sharipov and G. Bertoldo, *J. Vac. Sci. Technol. A* **23**, 531 (2005).
- 36) T. Sugawara and T. Takami, in preparation.